

On the multi- \mathbf{q} characteristics of magnetic ground states of honeycomb cobalt oxides

Yuchen Gu,¹ Xianghong Jin,¹ and Yuan Li^{1,2,*}

¹*International Center for Quantum Materials, School of Physics, Peking University, Beijing 100871, China*

²*Beijing National Laboratory for Condensed Matter Physics,
Institute of Physics, Chinese Academy of Sciences, Beijing 100190, China*

(Dated: January 27, 2025)

The Kitaev honeycomb model has received significant attention for its exactly solvable quantum spin liquid ground states and fractionalized excitations. For realizing the model, layered cobalt oxides have been considered a promising platform. Yet, in contrast to the conventional wisdom about single- \mathbf{q} zigzag magnetic order inferred from previous studies of the Na_2IrO_3 and $\alpha\text{-RuCl}_3$ candidate materials, recent experiments on two of the representative honeycomb cobalt oxides, hexagonal $\text{Na}_2\text{Co}_2\text{TeO}_6$ and monoclinic $\text{Na}_3\text{Co}_2\text{SbO}_6$, have uncovered evidence for more complex multi- \mathbf{q} variants of the zigzag order. This review surveys on experimental strategies to distinguish between single- and multi- \mathbf{q} orders, along with the crystallographic symmetries of the cobalt oxides in comparison to the previously studied systems. General formation mechanism of multi- \mathbf{q} order is also briefly discussed. The goal is to provide some rationales for examining the relevance of multi- \mathbf{q} order in the honeycomb cobalt oxides, along with its implications on the microscopic model of these intriguing quantum magnets.

1. INTRODUCTION

Quantum spin liquid (QSL) is a novel phase of matter in an interacting quantum many-body system [1, 2]. Originating from the idea of the resonating valence bond concept [3], QSL has garnered widespread interest partly due to the suggestion of P. W. Anderson that resonating valence bonds may be the essence of superconducting pairing in the cuprates [4]. A QSL phase does not exhibit spontaneous symmetry breaking even at the lowest temperatures, and features long-range entanglement and fractional quantum excitations [5]. Low dimensionality, magnetic frustration, and strong quantum fluctuations are generally believed to facilitate the formation of QSLs [6]. These considerations are fused into the Kitaev honeycomb model [7]. The model, which is defined on a two-dimensional honeycomb lattice with spin-1/2 degrees of freedom and frustrated bond-dependent Ising interactions, has exactly solvable QSL ground states and fractionalized excitations.

A strategy for materializing the Kitaev model was first proposed by G. Jackeli and G. Khaliullin in spin-orbit coupled Mott insulators based on selected transition-metal ions [8]. Over the past decade and a half [9–11], extensive research efforts have gone into 5*d*-electron iridium-based [12], 4*d*-electron ruthenium-based [13], and most recently 3*d*-electron cobalt-based compounds [14–18]. However, the candidate compounds almost always develop long-range magnetic order at low temperatures when the role of disorder is minimized [9, 19–21], so the presence of non-Kitaev interactions is evident [12, 22–28]. The optimistic thinking is that, when the non-Kitaev terms are sufficiently small and only acting as perturbations to the Kitaev model, it would still be possible to suppress the long-range order formation through external tuning [16, 29, 30]. A commonly considered non-

Kitaev term is the isotropic Heisenberg interaction between nearest neighbors. In this context, the 3*d* cobalt-based systems are considered favorable, because of a cancellation mechanism to suppress such Heisenberg interactions [14–16].

Deriving from the conventional wisdom attained from studying the 4*d* and 5*d* materials [31–33], and following the common practice of using single- \mathbf{q} ansatz in the interpretation of diffraction data [19–21], the magnetic ground state in some of the cobaltates had once been accepted to be the single- \mathbf{q} zigzag order [17, 34, 35]. However, recent investigations on $\text{Na}_2\text{Co}_2\text{TeO}_6$ and $\text{Na}_3\text{Co}_2\text{SbO}_6$ have uncovered evidence for multi- \mathbf{q} order, which can be easily mistaken into the zigzag order with random domain distribution [36–41].

In this mini review, we present an overview of topics pertinent to the formation mechanism of multi- \mathbf{q} magnetic order in solids, ranging from crystallographic symmetry considerations to microscopic interactions, as well as experimental methods that can directly or indirectly indicate the existence of such order. It is hoped that such information will provide orientation for future work to assess the relevance of multi- \mathbf{q} magnetic order on a more equal footing as single- \mathbf{q} order, in candidate Kitaev materials and beyond, in order to constrain theoretical models with concrete characteristics of the magnetic ground state.

2. SINGLE- \mathbf{Q} ORDER UNDER LATTICE ROTATIONAL SYMMETRY

The formation of magnetic order leads to spontaneous symmetry breaking from the paramagnetic phase. Accurate information about the crystallographic symmetry is thus crucial for understanding the symmetry of the magnetic ground state. It is particularly important to ex-

amine the transformation of single- \mathbf{q} order's propagation vector under the crystallographic symmetry operations, in order to reveal whether it may have a multi- \mathbf{q} variant. A recent review [42] provides an excellent summary of the crystallographic and magnetic symmetries for the candidate Kitaev materials.

Na_2IrO_3 [12, 43] and $\alpha\text{-RuCl}_3$ [31] are the most extensively studied candidate Kitaev materials in the $5d$ and $4d$ categories, respectively. Na_2IrO_3 is established to have a monoclinic $C2/m$ structure through x-ray diffraction on single crystals with a low concentration of stacking faults [44]. In the case of $\alpha\text{-RuCl}_3$, extensive research has consistently identified its room-temperature structure as monoclinic $C2/m$ [31, 45]. However, recent studies have revealed a structural phase transition from $C2/m$ to rhombohedral $R\bar{3}$ upon cooling below about 150 K [46–49]. The completeness of this transition, along with thermal transport properties in the low-temperature phase, is highly sensitive to stacking faults in the crystals [47].

The propagation vectors in both Na_2IrO_3 and $\alpha\text{-RuCl}_3$ are characterized by the M -point of the pseudo-hexagonal two-dimensional (2D) Brillouin zone of the honeycomb lattice that is passed through by the C_2 -symmetric \mathbf{b} axis, $\mathbf{q} = (0, 1, 1/2)$ [33] and $(0, 1, 1/3)$ [31] in the monoclinic notation, respectively (the difference is in the stacking of the ordered moments along the \mathbf{c} axis). Because the 2D wave vector $(0, 1)$ is unique and invariant under the monoclinic symmetry operations (Fig. 1), the single- \mathbf{q} order has no multi- \mathbf{q} variant, and its formation does not necessitate any spontaneous breaking of the lattice rotational symmetry. This understanding in the context of $\alpha\text{-RuCl}_3$, however, relies on the low-temperature crystal structure being monoclinic. If the genuine crystal structure is $R\bar{3}$ [46–49], the formation of the single- \mathbf{q} order may have observable consequences related to the broken C_3 rotational symmetry.

-	space group	wave vector (r.l.u.)	Refs.
Na_2IrO_3	$C2/m$	$(0, 1, 1/2)$	[33, 44]
$\alpha\text{-RuCl}_3$	$C2/m$ or $R\bar{3}$	$(0, 1, 1/3)$ ($C2/m$)	[31, 47]
$\text{BaCo}_2(\text{AsO}_4)_2$	$R\bar{3}$	$(0.27, 0, -1.31)$	[50, 51]
$\text{Na}_2\text{Co}_2\text{TeO}_6$	$P6_322$	$(1/2, 0, 0)$	[19, 20]
$\text{Na}_2\text{Co}_2\text{TeO}_6$ (m)	$C2/m$	$(\pm 1/2, 1/2, 0)$	[52]
$\text{Na}_3\text{Co}_2\text{SbO}_6$	$C2/m$	$(\pm 1/2, 1/2, 0)$	[21]

TABLE I. Space groups and magnetic propagation wave vectors of some candidate Kitaev materials. The wave vector of $\alpha\text{-RuCl}_3$ employs the monoclinic notation.

The $3d$ cobaltates can be thought of as high-spin counterparts to the $5d$ and $4d$ systems [14, 15, 18]. The candidate materials $\text{BaCo}_2(\text{AsO}_4)_2$ [50, 53], $\text{Na}_2\text{Co}_2\text{TeO}_6$ [19, 54], $\text{Na}_2\text{Co}_2\text{TeO}_6$ (m) (a monoclinic polymorph) [52]

and $\text{Na}_3\text{Co}_2\text{SbO}_6$ [21, 54] belong to the space groups $R\bar{3}$, $P6_322$, $C2/m$, and $C2/m$, respectively. The magnetic order in $\text{BaCo}_2(\text{AsO}_4)_2$ is incommensurate, with $\mathbf{q} = (0.27, 0, -1.31)$ [51, 55], distinct from the other candidate materials. Because of the complexity brought about by the incommensurability, the order's single- versus multi- \mathbf{q} nature has not been closely examined in the literature. Nevertheless, we note that the system's high rhombohedral symmetry would in principle allow the order to have multi- \mathbf{q} variants. The magnetic order in $\text{Na}_2\text{Co}_2\text{TeO}_6$ and $\text{Na}_3\text{Co}_2\text{SbO}_6$, presumed here to be single- \mathbf{q} , are characterized by commensurate 2D wave vectors at the M -point of the (pseudo)hexagonal Brillouin zone [19–21]. As shown in Fig. 1, the crystal structure of hexagonal $\text{Na}_2\text{Co}_2\text{TeO}_6$ has C_6 symmetry about the \mathbf{c} axis, which introduces three symmetry-related orientational domains that are energetically degenerate, all breaking the lattice rotational symmetry. The cases of monoclinic $\text{Na}_3\text{Co}_2\text{SbO}_6$ and $\text{Na}_2\text{Co}_2\text{TeO}_6$ (m) are different. While they share the same monoclinic structural symmetry as Na_2IrO_3 and $\alpha\text{-RuCl}_3$ (at room temperature), the pertinent M -point is not passed through by the monoclinic C_2 axis [21, 40, 56] (Fig. 1). As a result, the single- \mathbf{q} order would break all lattice rotational symmetry. The crystallographic space group and magnetic wave vectors of different compounds are summarized in table I.

As an aside, traditionally, magnetism in candidate Kitaev materials is described based on localized magnetic moments on the honeycomb lattice, as they are formed by the atomic spin-orbit coupled $J_{\text{eff}} = \frac{1}{2}$ pseudospins. However, such an ionic picture has been challenged in honeycomb iridium and ruthenium oxides [57–59], based on *ab initio* calculations which showed that the electronic band width due to inter-site hopping is comparable to

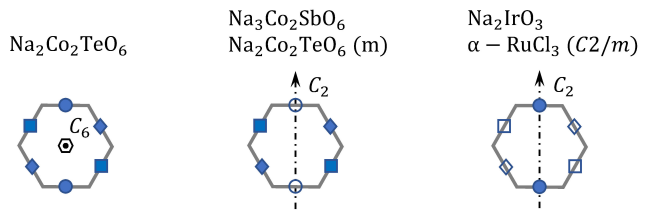


FIG. 1. Magnetic diffraction pattern of different compounds within the first 2D hexagonal Brillouin zone, *i.e.*, without considering the L components. $\text{Na}_2\text{Co}_2\text{TeO}_6$ features three sets of diffraction peaks which are linked by the C_3 rotation. These peaks are produced either together as Fourier components of a triple- \mathbf{q} magnetic order, or separately by three types of single- \mathbf{q} magnetic domains. Although $\text{Na}_2\text{Co}_2\text{TeO}_6$ (m), $\text{Na}_3\text{Co}_2\text{SbO}_6$, Na_2IrO_3 and $\alpha\text{-RuCl}_3$ all possess $C2/m$ space-group symmetry and have a C_2 symmetry axis along $(0, K, 0)$ at room temperature, only $\text{Na}_2\text{Co}_2\text{TeO}_6$ (m) and $\text{Na}_3\text{Co}_2\text{SbO}_6$ have two different sets of symmetry-related magnetic diffraction peaks. Notably, the exact lattice symmetry of $\alpha\text{-RuCl}_3$ at low temperatures remains a topic of ongoing discussion.

the Hubbard repulsion U . It is proposed that an alternative, more accurate low-energy description of the electronic structure involves a linear combination of six t_{2g} atomic orbitals on each hexagon of the honeycomb lattice, dubbed quasi-molecular orbitals (QMOs, in analogy with benzene molecules). While the precise electronic structure has remained a subject of debate [60–66], it is argued that the magnetic order in Na_2IrO_3 can also be understood from the QMO point of view [57]. We believe that whether such order may generally be single- or multi- \mathbf{q} (which in turn depends on the lattice symmetry) warrants further investigation, because the electron itinerancy behind QMO formation also promotes higher-order spin interactions in an ionic picture. As discussed in the next section, such higher-order interactions may be intimately linked to the stabilization of multi- \mathbf{q} order.

3. MULTI- \mathbf{Q} ORDER: PREVIOUS EXAMPLES

In crystals with sufficiently high rotational symmetry, conventional single- \mathbf{q} magnetic order can break the original rotational symmetry when the symmetry operations do not leave the ordering wave vector invariant. In these cases, a natural way to restore the symmetry is to conceptualize a multi- \mathbf{q} variant of the magnetic order, which inherently respects the full rotational symmetry of the material’s paramagnetic state. Multi- \mathbf{q} magnetic order can be viewed as the vector sum of all symmetry-equivalent single- \mathbf{q} components generated by the action of the material’s rotational symmetry operations. This summation typically results in a spin configuration that is non-collinear or even non-coplanar, even when the spins in each individual single- \mathbf{q} component are collinear (as long as they are not parallel to the rotational symmetry axis broken by the single- \mathbf{q} order). This distinguishing feature sets multi- \mathbf{q} magnetic order apart from conventional single- \mathbf{q} structures, offering richer, often more complex, magnetic textures. Before we discuss the subject of multi- \mathbf{q} magnetic order in the honeycomb cobaltates, it is useful to survey the formation mechanism and experimental determination of multi- \mathbf{q} order in previously studied materials.

In magnetic Hamiltonian with bilinear spin interactions, single- and multi- \mathbf{q} magnetic orders are often found to be degenerate in their semiclassical energy [38, 67]. As a result, thermal, quantum and quenched disorders [67–72] become important factors for selecting the magnetic ground state. A well-known form of multi- \mathbf{q} magnetic order is the skyrmion lattice [73, 74], which has been found in a variety of cubic and hexagonal magnetic metals with potential for spintronics applications [75–77]. Skyrmion lattices are believed to be stabilized by the joint effects of thermal fluctuations, external magnetic fields, Dzyaloshinskii-Moriya interactions, and magnetization amplitude variations in non-centrosymmetric

metallic magnets [78].

Multi- \mathbf{q} magnetic order has also been experimentally observed and theoretically studied in a variety of centrosymmetric systems. Representative materials include cubic [79, 80] and tetragonal systems [81–87] (notably, some of the multi- \mathbf{q} order in tetragonal systems are collinear, with spins parallel to the C_4 axis). In these systems, due to the presence of inversion symmetry, Dzyaloshinskii-Moriya interactions are no longer a key driving force, and magnetic frustration and/or spin anisotropy may play an important role [67, 72, 88–94]. In addition, the effectiveness of long-range (such as dipole-dipole or conduction electron-mediated) and higher-order spin interactions (such as biquadratic and multi-spin interactions) in stabilizing multi- \mathbf{q} magnetic order becomes highlighted in recent studies [38, 77, 80, 95–102]. While higher-order interactions in metallic magnets can arise from the interplay between conduction electrons and local moments within a Kondo-lattice picture [96, 103–105], they can also be understood as a natural consequence of higher-order expansion of the Hubbard model [106, 107]. It therefore seems that the presence of higher-order interactions may be considered a universal driving force for the formation of multi- \mathbf{q} magnetic order in both metallic and insulating systems.

Distinguishing between rotational symmetry-breaking single- \mathbf{q} order and its symmetry-preserving multi- \mathbf{q} variant can be challenging in conventional diffraction experiments [108, 109]. This is because, in both scenarios, magnetic diffraction intensities at the rotational symmetry-related \mathbf{q} vectors are expected to be nearly equal. The equality is intrinsic to multi- \mathbf{q} order, but extrinsic in the case of single- \mathbf{q} order due to randomized domain population. A viable strategy to differentiate the two is hence to create an unequal domain population in the latter case, by “training” the sample with external symmetry-breaking conditions. An example of this is displayed in Fig. 2, where the magnetic diffraction peaks from a single crystal of CeRh_2Si_2 are compared after cooling the sample with and without uniaxial compression [87]. The compression perturbs the symmetry of the Hamiltonian and cause single- \mathbf{q} domains to have different likelihoods of formation, resulting in variations in the corresponding magnetic diffraction intensities [Fig. 2(a-b)]. In contrast, the diffraction intensities associated with the symmetry-preserving multi- \mathbf{q} order are relatively insensitive to the compression [Fig. 2(c)]. In this way, the single- (between 25 K and 36 K) and multi- \mathbf{q} (below 25 K) nature of the ordered states can be distinguished. Similar experiments using strain or magnetic fields to “detwin” single- \mathbf{q} domains can be found for elucidating the multi- \mathbf{q} nature of magnetic order in a variety of materials, *i.e.*, based on the lack of detwinning effects [77, 85, 87, 110].

It is important to note that even a multi- \mathbf{q} order may break some (but not all) of the rotational symmetry [109]. A notable example of this is found in cubic SrFeO_3 [79], as

demonstrated by the measurement data in Fig. 3. Similar to the previous example, a magnetic field is applied upon cooling the sample, in order to alter the domain population indicated by the intensities of different magnetic Bragg peaks. The system is in a quadruple- \mathbf{q} ordered state in phase II [Fig. 3(a,c)], as manifested by the absence of clear field-training effects because the more stable quadruple- \mathbf{q} order preserves the full rotational symmetry of the cubic crystal. In phase I below 80 K, however, the more stable magnetic order becomes double- \mathbf{q} , which allows for the development of orientational domains that are trainable by the field. The training field can be applied either upon the initial cooling [Fig. 3(a)], or at low temperatures after zero-field cooling [Fig. 3(b)] as long as the field is sufficiently large, and the training effect persists even after the field is later removed. The training mechanism can be understood as follows. Without an external field, the double- \mathbf{q} order naturally develops in a total of 12 randomly distributed domains, each featuring the combinations of two wave vectors among q_1 , q_2 , q_3 and q_4 (and with time-reversal twins). In a

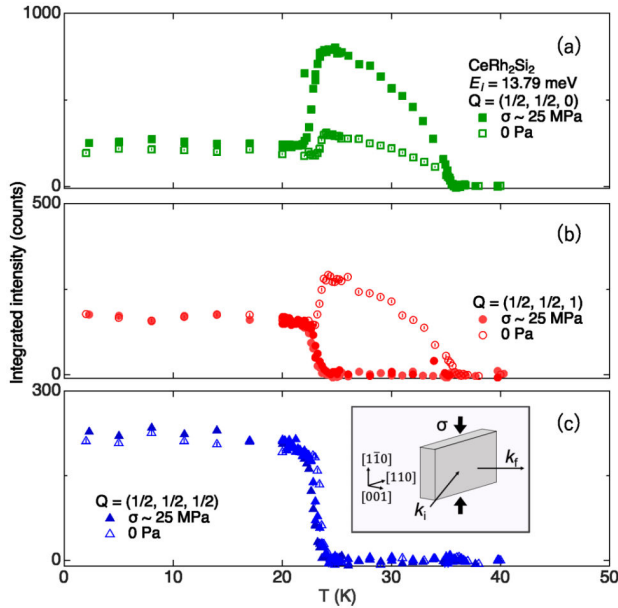


FIG. 2. Temperature dependence of magnetic neutron diffraction intensity in a single crystal of CeRh_2Si_2 (inset) cooled down with and without uniaxial stress, measured at various wave vectors: (a) $\mathbf{Q} = \mathbf{q} = (1/2, 1/2, 0)$, (b) $\mathbf{Q} = (1/2, 1/2, 1)$, which corresponds to $\mathbf{q} = (1/2, -1/2, 0)$ (measured from $\mathbf{G} = (0, 1, 1)$, due to the body-centered structure), and (c) $\mathbf{Q} = \mathbf{q} = (1/2, 1/2, 1/2)$. The first two \mathbf{q} 's have non-zero intensity in both the single- (between $T_{N1} = 36$ K and $T_{N2} = 25$ K) and multi- \mathbf{q} magnetic states (below T_{N2}), whereas the third \mathbf{q} exclusively characterizes the multi- \mathbf{q} state. The uniaxial compression σ , applied along the $(1, -1, 0)$ direction, favors the formation of the single- \mathbf{q} domain in (a) at the cost of the one in (b), but does not strongly affect the multi- \mathbf{q} order. The figure is reproduced from [87].

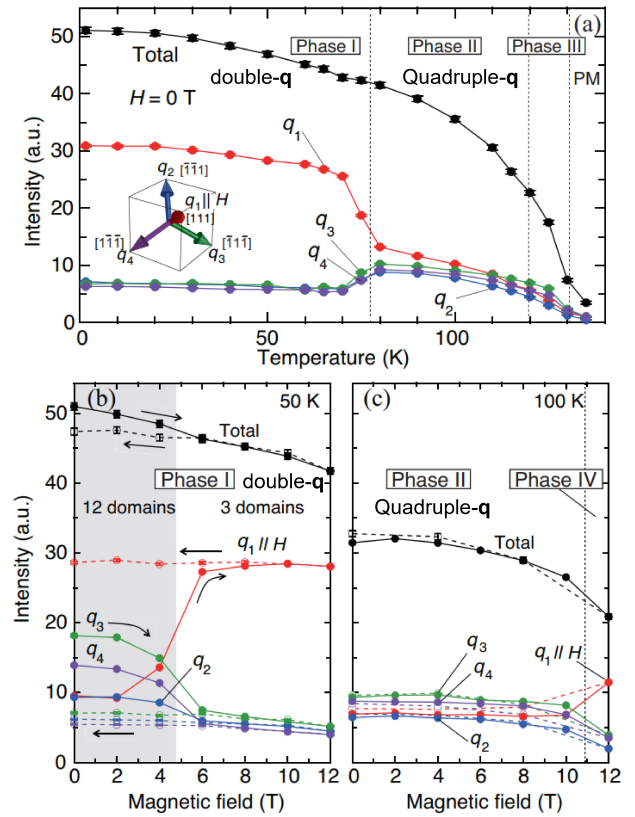


FIG. 3. (a) Temperature dependence of magnetic intensities measured at \mathbf{q}_i ($i = 1-4$) in zero field, after field-cooling the sample to the lowest temperature. (b) and (c) Magnetic field dependence of the scattering intensities measured in the double- \mathbf{q} phase I and the quadruple- \mathbf{q} phase II, respectively. The data with solid lines and broken lines were measured on increasing and decreasing the field along $[111]$, respectively. All the data were measured after zero-field cooling from room temperature. The figure is reproduced from [79].

training field, one of the wave vectors (say q_1) becomes favored over the other three, such that three of the twelve domains ($q_1 + q_2$, $q_1 + q_3$, and $q_1 + q_4$) are preferred. This makes the double- \mathbf{q} order's diffraction intensities at the unfavored wave vectors remain non-zero and amount to about one third of that at the favored wave vector [79].

Multi- \mathbf{q} states can also be identified through specific characteristics accessible in diffraction measurements without training the sample. One approach is to search for higher-order harmonic peaks, which can be interpreted as the coherent superposition of distinct \mathbf{q} components [86, 111]. However, this method may sometimes be confused with multiple scattering phenomena. Additionally, it has been suggested that under certain conditions, specific multi- \mathbf{q} states may exhibit zero intensity at the positions of higher-order harmonic peaks [100]. Another approach involves detecting associated structural symmetry breaking, which reflects magnetoelastic coupling effects in the rotational symmetry-breaking single- \mathbf{q}

state [82, 83]. Although high-resolution X-ray or neutron scattering techniques are required for this purpose due to the typically small induced lattice distortions, symmetry sensitive probes such as Raman scattering (for observing phonon splitting [112]) may be used as complementary methods.

Further signatures of multi- \mathbf{q} magnetic states may be found in the local spin orientations. As the electronic magnetic moments can affect the nuclear moments via the hyperfine coupling, they can be detected by nuclear technologies such as γ -ray emission [108] and Mössbauer spectroscopy [81, 114, 117]. Moreover, in some special cases, multi- \mathbf{q} states may be recognized through spin-polarized scanning tunnelling microscopy [118, 119] and nuclear magnetic resonance (NMR) [120]. In addition to static properties, multi- \mathbf{q} states can also leave signatures in the spin dynamics, which can be measured by inelastic neutron scattering (INS) [80, 113, 115, 116]. Evidence for multi- \mathbf{q} states may be obtained by either fitting the excitation spectrum [80, 113, 115] or scrutinizing their characteristic behavior that are distinct between single- and multi- \mathbf{q} states [116]. Table II summarizes how multi- \mathbf{q} magnetic ground states have been experimentally indicated in a variety of compounds.

4. EVIDENCE FOR MULTI-Q ORDER IN HONEYCOMB COBALT OXIDES

As discussed in Section 2 and illustrated in Fig. 1, the crystallographic symmetries of $\text{Na}_2\text{Co}_2\text{TeO}_6$ and $\text{Na}_3\text{Co}_2\text{SbO}_6$ are compatible with M -point magnetic order in either single- or multi- \mathbf{q} form. To tell which of these scenarios is more likely to be correct, single-crystal neutron diffraction experiments have recently been performed with in-plane magnetic fields in both $\text{Na}_2\text{Co}_2\text{TeO}_6$ [39] and $\text{Na}_3\text{Co}_2\text{SbO}_6$ [40]. Here we only focus on the training effects of the fields on the magnetic domains, as have been discussed in the previous Section.

In $\text{Na}_2\text{Co}_2\text{TeO}_6$, the single- \mathbf{q} magnetic structure (or single- \mathbf{q} component in a multi- \mathbf{q} structure) has been constrained [19, 20] to have the in-plane component of magnetic moments in each zigzag chain ferromagnetically aligned parallel to the chain, *i.e.*, perpendicular to \mathbf{q} . The moments are further canted towards the \mathbf{c} axis in an alternating fashion between the chains. Assuming that the multi- \mathbf{q} variant of the magnetic structure preserves all of the crystallographic rotational symmetries, one can infer its in-plane magnetic moment arrangement by summing up three single- \mathbf{q} components 120° from each other [36, 39], which results in an ordering pattern with spin “vortices” as displayed in Fig. 4(a).

In the recent experiments reported in Ref. 39, the magnetic domains in $\text{Na}_2\text{Co}_2\text{TeO}_6$ were trained either at the lowest temperature (2 K) up to a maximal field of 10 T, or upon cooling from the paramagnetic state in a 10 T field,

in a field geometry as shown in Fig. 4(a). Figures 4(b) and (c) present the evolution of magnetic Bragg peak intensities at $M_1 = (0.5, 0, 1)$ and $M_2 = (0, 0.5, 1)$, respectively, demonstrating the effect of training. As the training field was removed, the M_1 intensity recovered to about 2/3 of the value originally observed after zero-field cooling, whereas the M_2 intensity returned to the original value without a significant difference. These results showed that the training process had failed to eliminate the formation of any presumed, energetically unfavored single- \mathbf{q} domains. While the 1/3 intensity decrease at M_1 might indicate a partial suppression of the corresponding single- \mathbf{q} domain, it was found that the lost intensity (measured at integer $L = 1$) was redistributed into rod-like magnetic diffuse scattering along the \mathbf{c}^* axis, rather than into diffraction signals at other M points. In other words, while the training was able to affect the magnetic correlation length across the honeycomb layers, there was no indication for a repopulation of single- \mathbf{q} orientational domains within the layers [39]. These observations were in favor of a triple- \mathbf{q} magnetic ground state in $\text{Na}_2\text{Co}_2\text{TeO}_6$. The only remaining alternative possibility was that there existed unidentified structural pinning effects, such as frozen-in uniaxial strains, which are randomly distributed in the samples yet sufficiently strong to overrule the effects of the magnetic fields. This issue was addressed in a more recent study [121], where an emergent effect arising from the spin vorticity [Fig. 4(a)] was further observed with optical Faraday rotations.

The experimental situation in $\text{Na}_3\text{Co}_2\text{SbO}_6$ is similar. Here, the question is between single- and double- \mathbf{q} scenarios. The double- \mathbf{q} magnetic ground state [40] features a non-collinear arrangement of the in-plane magnetic moments [Fig. 4(d)], but it has no spin vorticity because of the absence of a third magnetic propagating vector along \mathbf{b}^* . To differentiate between the two scenarios, the in-plane training field was applied in a low-symmetry direction as illustrated in Fig. 4(d). The measured magnetic Bragg peak [Fig. 4(e-g)] was at the propagating wave vector which would correspond to domains that are unfavored by the training field in the single- \mathbf{q} order scenario. The central finding was that the diffraction signal recovered after the training field was removed, even though the field was strong enough to fully suppress the order. Hence, the recovered signal was more likely a component of the full, double- \mathbf{q} order parameter, rather than being associated with a given type of single- \mathbf{q} domains. Similar to the case of $\text{Na}_2\text{Co}_2\text{TeO}_6$, the peak intensity was observed to decrease after the training, due to a broadening of the momentum profile of the diffraction signals [Fig. 4(f-g)] especially along the \mathbf{c}^* axis. After accounting for the broadening, the total intensity was found to be unaffected by the training [40].

A distinct characteristic of the multi- \mathbf{q} ordering patterns in Figs. 4(a) and (d) is that some of the sites are found to have smaller magnitudes of ordered moments

-	Crystal structure	Type	Stabilized by	Way to identify	Refs.
Nd	hexagonal	metal	N.A.	higher-order satellites	[111]
Mn–Ni alloy	face-centered cubic	metal	N.A.	γ -ray emission	[108]
USb	face-centered cubic	metal	N.A.	excitation spectrum	[113]
(U _{1-x} Pu _x)Sb	face-centered cubic	metal	N.A.	field detwinning	[110]
SrFeO ₃	simple cubic	metal	thermal fluctuations	field detwinning	[79]
Y ₃ Co ₈ Sn ₄	honeycomb	metal	four-spin interaction	field detwinning	[77]
MnTe ₂	simple cubic	semiconductor	DM interaction	Mössbauer	[114]
Co _{1/3} TaS ₂	triangular	metal	four-spin interaction	excitation spectrum	[115, 116]
Co _{1/3} NbS ₂	triangular	metal	four-spin interaction	Mössbauer	[117]
CeRh ₂ Si ₂	tetragonal	metal	biquadratic interaction	stress detwinning	[87]
GdRu ₂ Si ₂	tetragonal	metal	higher-order interaction	field detwinning	[85]
				higher-order satellites	[86]
(Sr _{1-x} Na _x /Ba _{1-x} K _x)Fe ₂ As ₂	tetragonal	superconductor	biquadratic interaction	diffraction & Mössbauer	[81–83]
Ba ₂ (Y/Lu)RuO ₆	cubic	insulator	biquadratic interaction	excitation spectrum	[80, 97]
Na ₂ Co ₂ TeO ₆	honeycomb	insulator	ring exchange	excitation spectrum	[36]
				field detwinning	[39]
Na ₃ Co ₂ SbO ₆	monoclinic honeycomb	insulator	N.A.	field detwinning	[40]

TABLE II. List of materials with reported multi- \mathbf{q} magnetic states, along with the key experimental indications.

than the rest. In Na₂Co₂TeO₆, the sites which have zero in-plane moments are expected to have ordered moments along the \mathbf{c} -axis, which give rise to the system's ferrimagnetic behavior [124] in the ordered state, and which can be understood as related to the spin canting [19, 20] in the individual zigzag components. However, the magnitude of these moments are not expected to be equal to the in-plane ones, because the system has pronounced overall easy-plane response to external fields [124]. In Na₃Co₂SbO₆, the zero-field magnetic structure has been fully determined through spin-polarized neutron diffraction [40], with varying moments on the lattice sites as shown in Fig. 4(d). The presence of these reduced ordered moments implies the persistence of spin dynamics deeply in the ordered state due to the systems' magnetic frustration and quantum fluctuations, which has been confirmed in recent muon spin relaxation measurements [125].

The above evidence for multi- \mathbf{q} magnetic order in Na₂Co₂TeO₆ and Na₃Co₂SbO₆ came from diffraction experiments. Historically, the likelihood of triple- \mathbf{q} order in Na₂Co₂TeO₆ was first revealed by inelastic neutron scattering experiments based on symmetry arguments [36]. As illustrated in the upper half of Fig. 5, in the zigzag scenario, the three orientational domains feature rectangular magnetic Brillouin zones that are rotated 120° from each other. As a result, in a large, co-aligned sample for inelastic neutron scattering, one expects to observe spin excitations from all three types of domains simultaneously, *e.g.*, with two types of dispersion relations seen on the momentum trajectory displayed in the lower half of

Fig. 5. The experimental spectra [36] strongly contradict this expectation, as only one branch of spin-wave dispersion is observed below 3 meV. The data are instead fully consistent with a triple- \mathbf{q} understanding of the magnetic order, which has a smaller hexagonal magnetic Brillouin zone (which corresponds to the overlapped colored region in the lower-left of Fig. 5).

Yet, it is important to note that such symmetry arguments alone might not be rigorous, as they cannot be used to rule out zigzag order formation under certain interaction parameter settings. For instance, when the interaction model has only Heisenberg interactions between the third-nearest neighbors (J_3), in which case the zigzag and triple- \mathbf{q} orders are degenerate classical ground states, the magnon dispersions of different zigzag domains are also degenerate. This degeneracy arises because the spin lattice is effectively decoupled into different sublattices, as detailed in a discussion presented in Ref. [126]. Such degeneracy is, however, not symmetry-enforced, as the absence of interactions between nearer neighbors than J_3 is a special requirement. When such interactions are present, the fitting of entire INS spectrum [126] (not just the lowest-energy branch) starting from a zigzag ground state, and considering the coexistence of multiple domains, has remained a challenge [34, 127, 128]. Spin-wave fitting based on a triple- \mathbf{q} ground state has yielded considerably more satisfactory results [38], further supporting the triple- \mathbf{q} scenario.

In addition to the neutron scattering efforts discussed above, indirect evidence for multi- \mathbf{q} magnetic order has been obtained by other experimental techniques. These

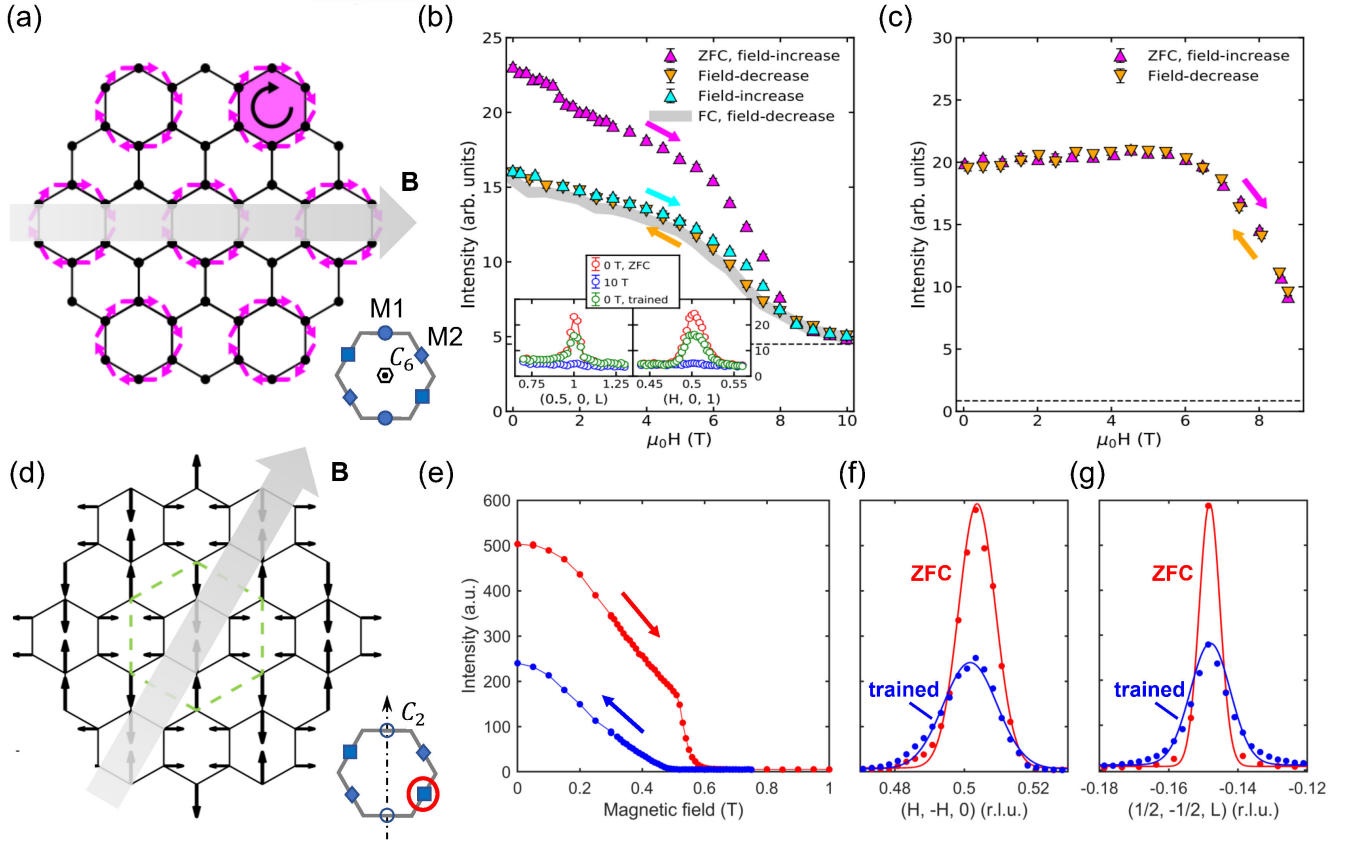


FIG. 4. (a) Schematic of triple- \mathbf{q} magnetic structure in $\text{Na}_2\text{Co}_2\text{TeO}_6$, constructed by summing up three zigzag components whose propagating wave vectors are different M -points of the Brillouin zone (inset). The direction of the applied magnetic field is unfavorable for the M_1 component. (b) and (c) Field evolution of magnetic Bragg peaks at $M_1 = (0.5, 0, 1)$ and $M_2 = (0, 0.5, 1)$ in $\text{Na}_2\text{Co}_2\text{TeO}_6$ at 2 K. Data displayed in the main panels are measured at the maximum of the peak profile (insets). Horizontal dashed lines indicate background level. (d) Schematic of double- \mathbf{q} magnetic structure in $\text{Na}_3\text{Co}_2\text{SbO}_6$, constructed by summing up two zigzag components that are related to each other by the C_2 rotational symmetry about the \mathbf{b} axis. With a magnetic field applied along the indicated low-symmetry direction, the zigzag component (circled in the inset) measured in (e-g) is expected to be unfavored. (e-g) Field evolution and training effect of the magnetic Bragg peak at $(1/2, -1/2, 0)$ in $\text{Na}_3\text{Co}_2\text{SbO}_6$ at 2 K. The figures are adapted from [39] and [40].

include null results in Raman scattering detection of phonon energy splitting in $\text{Na}_2\text{Co}_2\text{TeO}_6$ [36], which ought to be present if the magnetic order (in conjunction with magnetoelastic coupling) strongly breaks the lattice C_6 rotational symmetry about the \mathbf{c} axis, as well as nuclear magnetic resonance detection of the local internal fields in both $\text{Na}_2\text{Co}_2\text{TeO}_6$ [37] and $\text{Na}_3\text{Co}_2\text{SbO}_6$ [41]: a multi- \mathbf{q} magnetic ground state is expected to produce more complicated nuclear magnetic resonance spectra than a single- \mathbf{q} one.

5. IMPLICATIONS FOR THEORETICAL MODELS

Information about the magnetic ground state imposes strong constraints on microscopic magnetic model construction, providing critical insights into the underlying interactions. As discussed in Section. 3, the multi- \mathbf{q} order

in centrosymmetric itinerant magnets highlights the significant role of long-range and higher-order interactions, which in those cases naturally arise from the interplay between local moments and conduction electrons. In contrast, conventional models for Kitaev-candidate honeycomb cobaltates are based on the tight-binding Hubbard insulator framework, which in first-order approximation translates into spin Hamiltonians with only bilinear spin interactions (*e.g.*, Heisenberg and Kitaev interactions between two spins) [14–16, 129]. Within these models, the semi-classical energies of single- and multi- \mathbf{q} orders are usually degenerate [38, 67], but as displayed in Fig. 6, the ground state can become multi- \mathbf{q} order when higher-order spin interactions, or magnetic fields, are introduced [122, 123, 130, 131]. Indeed, in the case of $\text{Na}_2\text{Co}_2\text{TeO}_6$, a triple- \mathbf{q} ground state has been proposed to be stable in the presence of six-spin ring-exchange interactions, when the system is near a hidden $\text{SU}(2)$ -symmetric point in the parameter space of an extended Heisenberg-Kitaev-

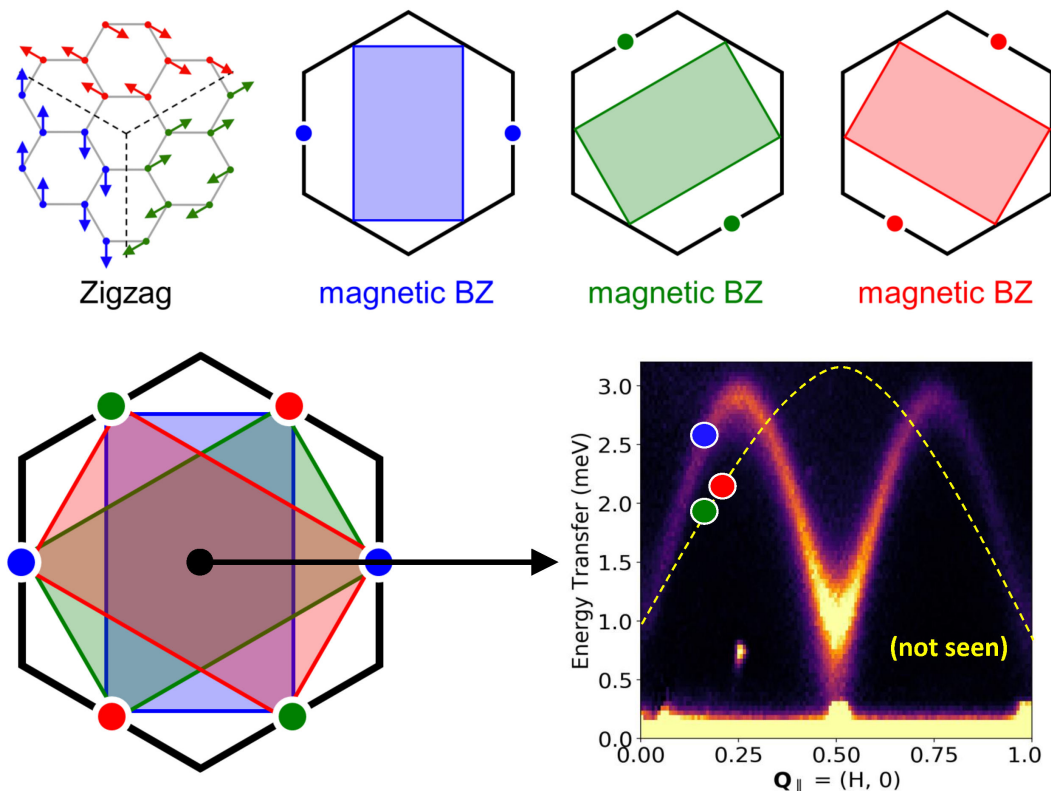


FIG. 5. Upper half: Three orientational domains of the zigzag order, along with their corresponding propagating wave vectors and magnetic Brillouin zones. Lower-left: Superposition of three types of magnetic Brillouin zones. When spin waves are measured along the momentum trajectory that connects two neighboring structural Brillouin zones (black arrow), two types of dispersion relations are expected to be seen, because the trajectory goes through magnetic zone centers three times in the “blue” domain, but only twice (plus zone corner once) in the “green” and “red” domains. Lower-right: Experimental spectra are consistent with the understanding that the momentum trajectory goes through magnetic zone centers three times, *i.e.*, without seeing the presumed contributions from the “green” and “red” zigzag domains, hence contradicting the zigzag scenario but consistent with the triple- \mathbf{q} scenario. The figure is adapted and modified from [36].

Gamma model [38]. Notably, the model is also able to provide a satisfactory description of the full experimental spin-wave spectrum.

Such multi-spin, higher-order interactions are considered to emerge from higher-order expansions of the tight-binding Hubbard model [38], and their presence underscores the critical role of electron hopping in Mott insulators. The significance of hopping be indicated by the dimensionless quantity t/U , where t and U are the inter-site hopping and on-site repulsion energies, respectively. Traditionally, hopping is expected to be less significant and more short-ranged in the cobalt oxides than in extended $5d$ - and $4d$ -electron systems [14–16]. However, recent detailed analysis of the electronic structure in one of the candidate materials, $\text{BaCo}_2(\text{AsO}_4)_2$ [132], suggests that the hopping energy may have been underestimated. Specifically, the direct xy/xy hopping $t' \sim -300$ meV dominates over superexchange hoppings between xz and yz orbitals via ligand p states $t \sim 50$ meV. Similar findings were also reported for $\text{Na}_2\text{BaCo}(\text{PO}_4)_2$ and other edge-sharing Co oxides [132–134]. This contradicts pre-

vious assumptions that ligand p state-mediated hopping is predominant in the cobaltates [16] as a key factor behind dominant Kitaev interactions. Another significant deviation is the notable hopping between the third nearest neighbors, which becomes substantial already at the DFT level [135]. According to inelastic neutron scattering results, the presence of third-nearest-neighbour spin interaction also appears to be a general characteristic of materials such as $\text{BaCo}_2(\text{AsO}_4)_2$, $\text{Na}_2\text{Co}_2\text{TeO}_6$ and $\text{Na}_3\text{Co}_2\text{SbO}_6$ [34, 38, 51, 126, 128].

The validity of microscopic models and their ground states can be further examined via the models’ ability to explain related experimental observations. It has been reported for $\text{Na}_2\text{Co}_2\text{TeO}_6$ that, before developing the well-known 3D magnetic order, the system exhibits an intermediate phase featuring an unusual form of 2D order [36]. This phase has recently been explained using a model with ring-exchange interactions [136]. Depending on the sign of the ring-exchange interactions, either a zigzag or a triple- \mathbf{q} ground state is favored, and they have intermediate “vestigial” phases in the forms of \mathbb{Z}_3 spin-nematic

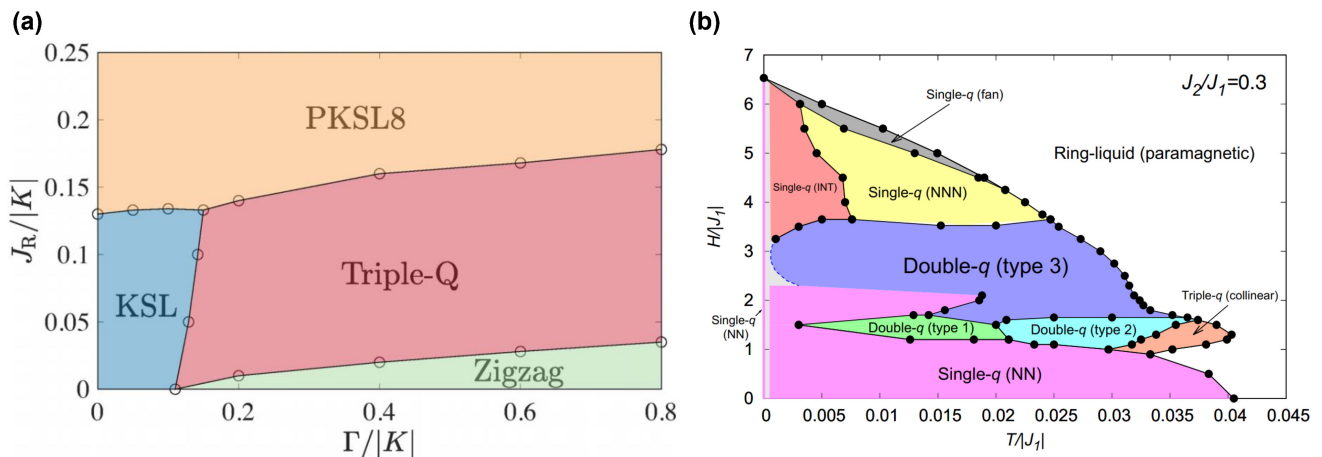


FIG. 6. (a) Phase diagram of the quantum $K - \Gamma - \Gamma' - J_R$ model for $K < 0$, $\Gamma > 0$, $J_R > 0$, and $\Gamma'/|K| = -0.05$ in the limit of large system size, calculated by variational Monte Carlo method. There are two different types of QSL phases: the KSL and the PKSL8, near the triple- \mathbf{q} phase. (b) The $H - T$ phase diagram of the $J_1 - J_2$ honeycomb-lattice Heisenberg model with $J_2/J_1 = 0.3$ determined by Monte Carlo simulation. The low-temperature light-gray region is the region where the thermalization cannot be achieved, while the zero-temperature limit can be identified based on the low-temperature expansion as a single- \mathbf{q} (NN) state. The dotted blue line representing the low-temperature phase boundary of the double- \mathbf{q} (type 3) state remains somewhat arbitrary. This figure is adapted from [122] and [123].

or \mathbb{Z}_4 spin-current density wave order, respectively. The experimentally observed vestigial phase in $\text{Na}_2\text{Co}_2\text{TeO}_6$ is consistent with the \mathbb{Z}_4 spin-current density wave order [136]. The order breaks lattice translational symmetry but preserves time-reversal symmetry, which explains why it does not lead to pronounced anomalies in magnetic susceptibility or NMR measurements [19, 20, 37, 124], but can be observed in specific heat and diffraction measurements [36, 39]. The same model can explain the experimentally observed ferrimagnetic net moment in the 3D ordered phase as well [124, 137].

6. SUMMARY & OUTLOOK

To summarize, we have reviewed how the possible existence of multi- \mathbf{q} order in magnetic materials can be experimentally addressed. This can be done either with reciprocal-space methods such as diffraction under external fields, with real-space methods such as NMR and STM. Current experimental evidence for such multi- \mathbf{q} magnetic order in the honeycomb cobaltates has followed these routes. The findings extend the relevance of multi- \mathbf{q} type of ordering from itinerant magnets to Mott insulators, promoting a re-examination of previously determined magnetic orders based on single- \mathbf{q} ansatz in similar systems. Since the presence of higher-order and long-range interactions probably plays a crucial role in stabilizing the multi- \mathbf{q} order, the results highlight the significance of electron itinerancy even in Mott insulator systems, challenging the conventional theoretical framework which leads to the prediction of dominant Kitaev interactions in the 3d honeycomb cobalt oxides.

Despite their likely substantial deviations from the Kitaev honeycomb model, the cobalt oxides retain the potential to host exotic quantum states. As displayed in Fig. 6(a), various spin liquid phases are predicted to emerge near the triple- \mathbf{q} phase [122]. Moreover, in these nearly ideal two-dimensional honeycomb magnets, theoretical studies suggest that a spin liquid ground state might emerge from competing interactions, particularly between the first and third nearest neighbors [51, 138–141]. The observation of a continuum scattering signal in $\text{BaCo}_2(\text{AsO}_4)_2$ via THz spectroscopy under a large \mathbf{c} -axis magnetic field may be indicative of such a state [142, 143]. The inferred unequal-magnitude spin distribution in the multi- \mathbf{q} states of $\text{Na}_2\text{Co}_2\text{TeO}_6$ and $\text{Na}_3\text{Co}_2\text{SbO}_6$ suggests that the classical order is suppressed by pronounced quantum fluctuations, a finding corroborated by muon spin relaxation measurements [125, 144]. While these materials finally develop antiferromagnetic order at low temperatures, the systems' tendency to form ferromagnetic correlations is not falling far behind and can be enhanced by external fields. Near the critical points between the quantum phases featuring these different magnetic correlations, exotic states with enhanced quantum fluctuations may emerge. In parallel to this optimistic view, it is equally important to acknowledge that seemingly novel observations might stem from relatively trivial origins such as disorders and lattice dynamics [145–149]. This highlights the need for careful interpretation of experimental data to distinguish genuine quantum phenomena from extrinsic effects.

We are grateful to our coworkers and colleagues for many fruitful collaboration and stimulating discussions.

The work at Peking University was supported by the National Basic Research Program of China (Grant No. 2021YFA1401901) and the NSF of China (Grant No. 12474138).

* yuan.li@iphy.ac.cn

- [1] C. Broholm, R. Cava, S. Kivelson, D. Nocera, M. Norman, and T. Senthil, Quantum spin liquids, *Science* **367**, eaay0668 (2020).
- [2] L. Balents, Spin liquids in frustrated magnets, *Nature* **464**, 199 (2010).
- [3] P. W. Anderson, Resonating valence bonds: A new kind of insulator?, *Materials Research Bulletin* **8**, 153 (1973).
- [4] P. W. Anderson, The resonating valence bond state in La_2CuO_4 and superconductivity, *science* **235**, 1196 (1987).
- [5] J. Wen, S.-L. Yu, S. Li, W. Yu, and J.-X. Li, Experimental identification of quantum spin liquids, *npj Quantum Materials* **4**, 12 (2019).
- [6] Y. Zhou, K. Kanoda, and T.-K. Ng, Quantum spin liquid states, *Rev. Mod. Phys.* **89**, 025003 (2017).
- [7] A. Kitaev, Anyons in an exactly solved model and beyond, *Ann. Phys.* **321**, 2 (2006).
- [8] G. Jackeli and G. Khaliullin, Mott Insulators in the Strong Spin-Orbit Coupling Limit: From Heisenberg to a Quantum Compass and Kitaev Models, *Phys. Rev. Lett.* **102**, 017205 (2009).
- [9] H. Takagi, T. Takayama, G. Jackeli, G. Khaliullin, and S. E. Nagler, Concept and realization of Kitaev quantum spin liquids, *Nat. Rev. Phys.* **1**, 264 (2019).
- [10] Y. Motome, R. Sano, S. Jang, Y. Sugita, and Y. Kato, Materials design of Kitaev spin liquids beyond the Jackeli-Khaliullin mechanism, *Journal of Physics: Condensed Matter* **32**, 404001 (2020).
- [11] S. Trebst and C. Hickey, Kitaev materials, *Physics Reports* **950**, 1 (2022).
- [12] J. Chaloupka, G. Jackeli, and G. Khaliullin, Kitaev-Heisenberg Model on a Honeycomb Lattice: Possible Exotic Phases in Iridium Oxides A_2IrO_3 , *Phys. Rev. Lett.* **105**, 027204 (2010).
- [13] K. W. Plumb, J. P. Clancy, L. J. Sandilands, V. V. Shankar, Y. F. Hu, K. S. Burch, H.-Y. Kee, and Y.-J. Kim, α - RuCl_3 : A spin-orbit assisted Mott insulator on a honeycomb lattice, *Phys. Rev. B* **90**, 041112 (2014).
- [14] H. Liu and G. Khaliullin, Pseudospin exchange interactions in d^7 cobalt compounds: Possible realization of the Kitaev model, *Phys. Rev. B* **97**, 014407 (2018).
- [15] R. Sano, Y. Kato, and Y. Motome, Kitaev-Heisenberg Hamiltonian for high-spin d^7 Mott insulators, *Phys. Rev. B* **97**, 014408 (2018).
- [16] H. Liu, J. Chaloupka, and G. Khaliullin, Kitaev Spin Liquid in 3d Transition Metal Compounds, *Phys. Rev. Lett.* **125**, 047201 (2020).
- [17] C. Kim, H.-S. Kim, and J.-G. Park, Spin-orbital entangled state and realization of Kitaev physics in 3d cobalt compounds: a progress report, *Journal of Physics: Condensed Matter* **34**, 023001 (2021).
- [18] H. Liu, Towards Kitaev spin liquid in 3d transition metal compounds, *Int. J. Mod. Phys. B* **35**, 2130006 (2021).
- [19] E. Lefrançois, M. Songvilay, J. Robert, G. Nataf, E. Jordan, L. Chaix, C. V. Colin, P. Lejay, A. Hadj-Azzem, R. Ballou, and V. Simonet, Magnetic properties of the honeycomb oxide $\text{Na}_2\text{Co}_2\text{TeO}_6$, *Phys. Rev. B* **94**, 214416 (2016).
- [20] A. K. Bera, S. M. Yusuf, A. Kumar, and C. Ritter, Zigzag antiferromagnetic ground state with anisotropic correlation lengths in the quasi-two-dimensional honeycomb lattice compound $\text{Na}_2\text{Co}_2\text{TeO}_6$, *Phys. Rev. B* **95**, 094424 (2017).
- [21] J.-Q. Yan, S. Okamoto, Y. Wu, Q. Zheng, H. D. Zhou, H. B. Cao, and M. A. McGuire, Magnetic order in single crystals of $\text{Na}_3\text{Co}_2\text{SbO}_6$ with a honeycomb arrangement of $3d^7 \text{Co}^{2+}$ ions, *Phys. Rev. Mater.* **3**, 074405 (2019).
- [22] J. Chaloupka, G. Jackeli, and G. Khaliullin, Zigzag Magnetic Order in the Iridium Oxide Na_2IrO_3 , *Phys. Rev. Lett.* **110**, 097204 (2013).
- [23] I. Kimchi and Y.-Z. You, Kitaev-Heisenberg- J_2 - J_3 model for the iridates A_2IrO_3 , *Phys. Rev. B* **84**, 180407 (2011).
- [24] Y. Sizyuk, C. Price, P. Wölfle, and N. B. Perkins, Importance of anisotropic exchange interactions in honeycomb iridates: Minimal model for zigzag antiferromagnetic order in Na_2IrO_3 , *Phys. Rev. B* **90**, 155126 (2014).
- [25] J. G. Rau, E. K.-H. Lee, and H.-Y. Kee, Generic spin model for the honeycomb iridates beyond the kitaev limit, *Phys. Rev. Lett.* **112**, 077204 (2014).
- [26] J. Chaloupka and G. Khaliullin, Magnetic anisotropy in the Kitaev model systems Na_2IrO_3 and RuCl_3 , *Phys. Rev. B* **94**, 064435 (2016).
- [27] S. M. Winter, Y. Li, H. O. Jeschke, and R. Valentí, Challenges in design of kitaev materials: Magnetic interactions from competing energy scales, *Phys. Rev. B* **93**, 214431 (2016).
- [28] I. Rousochatzakis, J. Reuther, R. Thomale, S. Rachel, and N. B. Perkins, Phase diagram and quantum order by disorder in the kitaev $K_1 - K_2$ honeycomb magnet, *Phys. Rev. X* **5**, 041035 (2015).
- [29] R. Yadav, N. A. Bogdanov, V. M. Katukuri, S. Nishimoto, J. Van Den Brink, and L. Hozoi, Kitaev exchange and field-induced quantum spin-liquid states in honeycomb α - RuCl_3 , *Scientific reports* **6**, 37925 (2016).
- [30] C. Hickey and S. Trebst, Emergence of a field-driven $U(1)$ spin liquid in the Kitaev honeycomb model, *Nat. Commun.* **10**, 530 (2019).
- [31] H. B. Cao, A. Banerjee, J.-Q. Yan, C. A. Bridges, M. D. Lumsden, D. G. Mandrus, D. A. Tennant, B. C. Chakoumakos, and S. E. Nagler, Low-temperature crystal and magnetic structure of α - RuCl_3 , *Phys. Rev. B* **93**, 134423 (2016).
- [32] X. Liu, T. Berlijn, W.-G. Yin, W. Ku, A. Tsvelik, Y.-J. Kim, H. Gretarsson, Y. Singh, P. Gegenwart, and J. P. Hill, Long-range magnetic ordering in Na_2IrO_3 , *Phys. Rev. B* **83**, 220403 (2011).
- [33] F. Ye, S. Chi, H. Cao, B. C. Chakoumakos, J. A. Fernandez-Baca, R. Custelcean, T. F. Qi, O. B. Korneta, and G. Cao, Direct evidence of a zigzag spin-chain structure in the honeycomb lattice: A neutron and x-ray diffraction investigation of single-crystal Na_2IrO_3 , *Phys. Rev. B* **85**, 180403 (2012).
- [34] M. Songvilay, J. Robert, S. Petit, J. A. Rodriguez-Rivera, W. D. Ratcliff, F. Damay, V. Balédent, M. Jiménez-Ruiz, P. Lejay, E. Pachoud, A. Hadj-Azzem, V. Simonet, and C. Stock, Kitaev interactions in

- the Co honeycomb antiferromagnets $\text{Na}_3\text{Co}_2\text{SbO}_6$ and $\text{Na}_2\text{Co}_2\text{TeO}_6$, *Phys. Rev. B* **102**, 224429 (2020).
- [35] A. M. Samarakoon, Q. Chen, H. Zhou, and V. O. Garlea, Static and dynamic magnetic properties of honeycomb lattice antiferromagnets $\text{Na}_2M_2\text{TeO}_6$, $M = \text{Co}$ and Ni , *Phys. Rev. B* **104**, 184415 (2021).
- [36] W. Chen, X. Li, Z. Hu, Z. Hu, L. Yue, R. Sutarto, F. He, K. Iida, K. Kamazawa, W. Yu, X. Lin, and Y. Li, Spin-orbit phase behavior of $\text{Na}_2\text{Co}_2\text{TeO}_6$ at low temperatures, *Phys. Rev. B* **103**, L180404 (2021).
- [37] C. H. Lee, S. Lee, Y. S. Choi, Z. H. Jang, R. Kalaivanan, R. Sankar, and K.-Y. Choi, Multistage development of anisotropic magnetic correlations in the Co-based honeycomb lattice $\text{Na}_2\text{Co}_2\text{TeO}_6$, *Phys. Rev. B* **103**, 214447 (2021).
- [38] W. G. F. Krüger, W. Chen, X. Jin, Y. Li, and L. Janssen, Triple- \mathbf{q} Order in $\text{Na}_2\text{Co}_2\text{TeO}_6$ from Proximity to Hidden-SU(2)-Symmetric Point, *Phys. Rev. Lett.* **131**, 146702 (2023).
- [39] W. Yao, Y. Zhao, Y. Qiu, C. Balz, J. R. Stewart, J. W. Lynn, and Y. Li, Magnetic ground state of the Kitaev $\text{Na}_2\text{Co}_2\text{TeO}_6$ spin liquid candidate, *Phys. Rev. Res.* **5**, L022045 (2023).
- [40] Y. Gu, X. Li, Y. Chen, K. Iida, A. Nakao, K. Munakata, V. O. Garlea, Y. Li, G. Deng, I. A. Zaliznyak, J. M. Tranquada, and Y. Li, In-plane multi- \mathbf{q} magnetic ground state of $\text{Na}_3\text{Co}_2\text{SbO}_6$, *Phys. Rev. B* **109**, L060410 (2024).
- [41] Z. Hu, Y. Chen, Y. Cui, S. Li, C. Li, X. Xu, Y. Chen, X. Li, Y. Gu, R. Yu, R. Zhou, Y. Li, and W. Yu, Field-induced phase transitions and quantum criticality in the honeycomb antiferromagnet $\text{Na}_3\text{Co}_2\text{SbO}_6$, *Phys. Rev. B* **109**, 054411 (2024).
- [42] V. O. Garlea and C. L. Sarkis, Review of honeycomb-based kitaev materials with zigzag magnetic ordering (2024), arXiv:2410.11083 [cond-mat.str-el].
- [43] Y. Singh and P. Gegenwart, Antiferromagnetic Mott insulating state in single crystals of the honeycomb lattice material Na_2IrO_3 , *Phys. Rev. B* **82**, 064412 (2010).
- [44] S. K. Choi, R. Coldea, A. N. Kolmogorov, T. Lancaster, I. I. Mazin, S. J. Blundell, P. G. Radaelli, Y. Singh, P. Gegenwart, K. R. Choi, S.-W. Cheong, P. J. Baker, C. Stock, and J. Taylor, Spin Waves and Revised Crystal Structure of Honeycomb Iridate Na_2IrO_3 , *Phys. Rev. Lett.* **108**, 127204 (2012).
- [45] R. D. Johnson, S. C. Williams, A. A. Haghighirad, J. Singleton, V. Zapf, P. Manuel, I. I. Mazin, Y. Li, H. O. Jeschke, R. Valentí, and R. Coldea, Monoclinic crystal structure of $\alpha\text{-RuCl}_3$ and the zigzag antiferromagnetic ground state, *Phys. Rev. B* **92**, 235119 (2015).
- [46] S. Mu, K. D. Dixit, X. Wang, D. L. Abernathy, H. Cao, S. E. Nagler, J. Yan, P. Lampen-Kelley, D. Mandrus, C. A. Polanco, L. Liang, G. B. Halász, Y. Cheng, A. Banerjee, and T. Berlijn, Role of the third dimension in searching for Majorana fermions in $\alpha\text{-RuCl}_3$ via phonons, *Phys. Rev. Res.* **4**, 013067 (2022).
- [47] H. Zhang, M. A. McGuire, A. F. May, H.-Y. Chao, Q. Zheng, M. Chi, B. C. Sales, D. G. Mandrus, S. E. Nagler, H. Miao, F. Ye, and J. Yan, Stacking disorder and thermal transport properties of $\alpha\text{-RuCl}_3$, *Phys. Rev. Mater.* **8**, 014402 (2024).
- [48] S. Park, S. Do, K.-Y. Choi, D. Jang, T. Jang, J. Schefer, C.-M. Wu, J. S. Gardner, S. Park, J.-H. Park, and S. Ji, Emergence of the Isotropic Kitaev Honeycomb Lattice $\alpha\text{-RuCl}_3$ and its magnetic properties, *Journal of Physics: Condensed Matter* (2024).
- [49] S. Kim, E. Horsley, C. Nelson, J. Ruff, and Y.-J. Kim, Re-investigation of Moment Direction in a Kitaev Material $\alpha\text{-RuCl}_3$, (2024), arXiv:2403.04176 [cond-mat.str-el].
- [50] L. Regnault, P. Burlet, and J. Rossat-Mignod, Magnetic ordering in a planar X-Y model: $\text{BaCo}_2(\text{AsO}_4)_2$, *Physica B+ C* **86**, 660 (1977).
- [51] T. Halloran, F. Desrochers, E. Z. Zhang, T. Chen, L. E. Chern, Z. Xu, B. Winn, M. Graves-Brook, M. B. Stone, A. I. Kolesnikov, Y. Qiu, R. Zhong, R. Cava, Y. B. Kim, and C. Broholm, Geometrical frustration versus Kitaev interactions in $\text{BaCo}_2(\text{AsO}_4)_2$, *Proceedings of the National Academy of Sciences* **120**, e2215509119 (2023).
- [52] E. Dufault, F. Bahrami, A. Streeter, X. Yao, E. Gonzalez, Q. Zhang, and F. Tafti, Introducing the monoclinic polymorph of the honeycomb magnet $\text{Na}_2\text{Co}_2\text{TeO}_6$, *Phys. Rev. B* **108**, 064405 (2023).
- [53] R. Zhong, T. Gao, N. P. Ong, and R. J. Cava, Weak-field induced nonmagnetic state in a Co-based honeycomb, *Science Advances* **6**, eaay6953 (2020).
- [54] L. Viciu, Q. Huang, E. Morosan, H. Zandbergen, N. Greenbaum, T. McQueen, and R. Cava, Structure and basic magnetic properties of the honeycomb lattice compounds $\text{Na}_2\text{Co}_2\text{TeO}_6$ and $\text{Na}_3\text{Co}_2\text{SbO}_6$, *J. Solid State Chem.* **180**, 1060 (2007).
- [55] L.-P. Regnault, C. Boullier, and J. Lorenzo, Polarized-neutron investigation of magnetic ordering and spin dynamics in $\text{BaCo}_2(\text{AsO}_4)_2$ frustrated honeycomb-lattice magnet, *Heliyon* **4**, e00507 (2018).
- [56] X. Li, Y. Gu, Y. Chen, V. O. Garlea, K. Iida, K. Kamazawa, Y. Li, G. Deng, Q. Xiao, X. Zheng, Z. Ye, Y. Peng, I. A. Zaliznyak, J. M. Tranquada, and Y. Li, Giant Magnetic In-Plane Anisotropy and Competing Instabilities in $\text{Na}_3\text{Co}_2\text{SbO}_6$, *Phys. Rev. X* **12**, 041024 (2022).
- [57] I. I. Mazin, H. O. Jeschke, K. Foyevtsova, R. Valentí, and D. I. Khomskii, Na_2IrO_3 as a Molecular Orbital Crystal, *Phys. Rev. Lett.* **109**, 197201 (2012).
- [58] K. Foyevtsova, H. O. Jeschke, I. I. Mazin, D. I. Khomskii, and R. Valentí, Ab initio analysis of the tight-binding parameters and magnetic interactions in Na_2IrO_3 , *Phys. Rev. B* **88**, 035107 (2013).
- [59] S. Streltsov, I. I. Mazin, and K. Foyevtsova, Localized itinerant electrons and unique magnetic properties of SrRu_2O_6 , *Phys. Rev. B* **92**, 134408 (2015).
- [60] H. Gretarsson, J. P. Clancy, X. Liu, J. P. Hill, E. Bozin, Y. Singh, S. Manni, P. Gegenwart, J. Kim, A. H. Said, D. Casa, T. Gog, M. H. Upton, H.-S. Kim, J. Yu, V. M. Katukuri, L. Hozoi, J. van den Brink, and Y.-J. Kim, Crystal-Field Splitting and Correlation Effect on the Electronic Structure of A_2IrO_3 , *Phys. Rev. Lett.* **110**, 076402 (2013).
- [61] I. I. Mazin, S. Manni, K. Foyevtsova, H. O. Jeschke, P. Gegenwart, and R. Valentí, Origin of the insulating state in honeycomb iridates and rhodates, *Phys. Rev. B* **88**, 035115 (2013).
- [62] B. H. Kim, T. Shirakawa, and S. Yunoki, From a quasi-molecular band insulator to a relativistic mott insulator in t_{2g}^5 systems with a honeycomb lattice structure, *Phys. Rev. Lett.* **117**, 187201 (2016).
- [63] B. H. Kim, G. Khaliullin, and B. I. Min, Electronic excitations in the edge-shared relativistic Mott insulator:

- Na_2IrO_3 , Phys. Rev. B **89**, 081109 (2014).
- [64] J.-I. Igarashi and T. Nagao, Collective excitations in Na_2IrO_3 , Journal of Physics: Condensed Matter **28**, 026006 (2015).
- [65] H. Suzuki, H. Gretarsson, H. Ishikawa, K. Ueda, Z. Yang, H. Liu, H. Kim, D. Kukusta, A. Yaresko, M. Minola, *et al.*, Spin waves and spin-state transitions in a ruthenate high-temperature antiferromagnet, Nature materials **18**, 563 (2019).
- [66] B. W. Lebert, S. Kim, B. H. Kim, S. H. Chun, D. Casa, J. Choi, S. Agrestini, K. Zhou, M. Garcia-Fernandez, and Y.-J. Kim, Nonlocal features of the spin-orbit exciton in Kitaev materials, Phys. Rev. B **108**, 155122 (2023).
- [67] S.-S. Diop, G. Jackeli, and L. Savary, Anisotropic exchange and noncollinear antiferromagnets on a noncentrosymmetric fcc half-Heusler structure, Phys. Rev. B **105**, 144431 (2022).
- [68] C. L. Henley, Ordering due to disorder in a frustrated vector antiferromagnet, Phys. Rev. Lett. **62**, 2056 (1989).
- [69] Q. Sheng and C. L. Henley, Ordering due to disorder in a triangular Heisenberg antiferromagnet with exchange anisotropy, Journal of Physics: Condensed Matter **4**, 2937 (1992).
- [70] R. Schick, T. Ziman, and M. E. Zhitomirsky, Quantum versus thermal fluctuations in the fcc antiferromagnet: Alternative routes to order by disorder, Phys. Rev. B **102**, 220405 (2020).
- [71] C. Liu, R. Yu, and X. Wang, Semiclassical ground-state phase diagram and multi- q phase of a spin-orbit-coupled model on triangular lattice, Phys. Rev. B **94**, 174424 (2016).
- [72] L. Seabra, P. Sindzingre, T. Momoi, and N. Shannon, Novel phases in a square-lattice frustrated ferromagnet: $\frac{1}{3}$ -magnetization plateau, helical spin liquid, and vortex crystal, Phys. Rev. B **93**, 085132 (2016).
- [73] S. Mühlbauer, B. Binz, F. Jonietz, C. Pfleiderer, A. Rosch, A. Neubauer, R. Georgii, and P. Böni, Skyrmion lattice in a chiral magnet, Science **323**, 915 (2009), <https://www.science.org/doi/pdf/10.1126/science.1166767>.
- [74] A. Bogdanov and A. Hubert, Thermodynamically stable magnetic vortex states in magnetic crystals, Journal of Magnetism and Magnetic Materials **138**, 255 (1994).
- [75] N. Kanazawa, Y. Onose, T. Arima, D. Okuyama, K. Ohoyama, S. Wakimoto, K. Kakurai, S. Ishiwata, and Y. Tokura, Large topological Hall effect in a short-period helimagnet mng, Phys. Rev. Lett. **106**, 156603 (2011).
- [76] S. Nakatsuji, N. Kiyohara, and T. Higo, Large anomalous Hall effect in a non-collinear antiferromagnet at room temperature, Nature **527**, 212 (2015).
- [77] R. Takagi, J. S. White, S. Hayami, R. Arita, D. Honecker, H. M. Rønnow, Y. Tokura, and S. Seki, Multiple- q noncollinear magnetism in an itinerant hexagonal magnet, Science Advances **4**, eaau3402 (2018).
- [78] U. K. Roessler, A. Bogdanov, and C. Pfleiderer, Spontaneous skyrmion ground states in magnetic metals, Nature **442**, 797 (2006).
- [79] S. Ishiwata, T. Nakajima, J.-H. Kim, D. S. Inosov, N. Kanazawa, J. S. White, J. L. Gavilano, R. Georgii, K. M. Seemann, G. Brandl, P. Manuel, D. D. Khalyavin, S. Seki, Y. Tokunaga, M. Kinoshita, Y. W. Long, Y. Kaneko, Y. Taguchi, T. Arima, B. Keimer, and Y. Tokura, Emergent topological spin structures in the centrosymmetric cubic perovskite SrFeO_3 , Phys. Rev. B **101**, 134406 (2020).
- [80] J. A. Paddison, H. Zhang, J. Yan, M. J. Cliffe, M. A. McGuire, S.-H. Do, S. Gao, M. B. Stone, D. Dahlbom, K. Barros, *et al.*, Cubic double perovskites host non-coplanar spin textures, npj Quantum Materials **9**, 48 (2024).
- [81] J. M. Allred, K. M. Taddei, D. E. Bugaris, M. J. Krogstad, S. H. Lapidus, D. Y. Chung, H. Claus, M. G. Kanatzidis, D. E. Brown, J. Kang, R. M. Fernandes, I. Eremin, S. Rosenkranz, O. Chmaissem, and R. Osborn, Double- q spin-density wave in iron arsenide superconductors, Nature Physics **12**, 493.
- [82] J. M. Allred, S. Avci, D. Y. Chung, H. Claus, D. D. Khalyavin, P. Manuel, K. M. Taddei, M. G. Kanatzidis, S. Rosenkranz, R. Osborn, and O. Chmaissem, Tetragonal magnetic phase in $\text{Ba}_{1-x}\text{K}_x\text{Fe}_2\text{As}_2$ from x-ray and neutron diffraction, Phys. Rev. B **92**, 094515 (2015).
- [83] K. M. Taddei, J. M. Allred, D. E. Bugaris, S. Lapidus, M. J. Krogstad, R. Stadel, H. Claus, D. Y. Chung, M. G. Kanatzidis, S. Rosenkranz, R. Osborn, and O. Chmaissem, Detailed magnetic and structural analysis mapping a robust magnetic C_4 dome in $\text{Sr}_{1-x}\text{Na}_x\text{Fe}_2\text{As}_2$, Phys. Rev. B **93**, 134510 (2016).
- [84] S. Kawarazaki, M. Sato, Y. Miyako, N. Chigusa, K. Watanabe, N. Metoki, Y. Koike, and M. Nishi, Ground-state magnetic structure of CeRh_2Si_2 and the response to hydrostatic pressure as studied by neutron diffraction, Phys. Rev. B **61**, 4167 (2000).
- [85] N. D. Khanh, T. Nakajima, S. Hayami, S. Gao, Y. Yamasaki, H. Sagayama, H. Nakao, R. Takagi, Y. Motome, Y. Tokura, *et al.*, Zoology of multiple- q spin textures in a centrosymmetric tetragonal magnet with itinerant electrons, Advanced Science **9**, 2105452 (2022).
- [86] G. D. A. Wood, D. D. Khalyavin, D. A. Mayoh, J. Bouaziz, A. E. Hall, S. J. R. Holt, F. Orlandi, P. Manuel, S. Blügel, J. B. Staunton, O. A. Petrenko, M. R. Lees, and G. Balakrishnan, Double- Q ground state with topological charge stripes in the centrosymmetric skyrmion candidate GdRu_2Si_2 , Phys. Rev. B **107**, L180402 (2023).
- [87] H. Saito, F. Kon, H. Hidaka, H. Amitsuka, C. Kwanghee, M. Hagihala, T. Kamiyama, S. Itoh, and T. Nakajima, In-plane anisotropy of single- q and multiple- q ordered phases in the antiferromagnetic metal CeRh_2Si_2 , Phys. Rev. B **108**, 094440 (2023).
- [88] T. Okubo, T. H. Nguyen, and H. Kawamura, Cubic and noncubic multiple- q states in the Heisenberg antiferromagnet on the pyrochlore lattice, Phys. Rev. B **84**, 144432 (2011).
- [89] T. Okubo, S. Chung, and H. Kawamura, Multiple- q states and the skyrmion lattice of the triangular-lattice Heisenberg antiferromagnet under magnetic fields, Phys. Rev. Lett. **108**, 017206 (2012).
- [90] Y. Kamiya and C. D. Batista, Magnetic vortex crystals in frustrated Mott insulator, Phys. Rev. X **4**, 011023 (2014).
- [91] S. Hayami, S.-Z. Lin, and C. D. Batista, Bubble and skyrmion crystals in frustrated magnets with easy-axis anisotropy, Phys. Rev. B **93**, 184413 (2016).
- [92] S. Hayami and Y. Motome, Effect of magnetic anisotropy on skyrmions with a high topological number

- in itinerant magnets, *Phys. Rev. B* **99**, 094420 (2019).
- [93] S. Hayami and Y. Motome, Noncoplanar multiple- Q spin textures by itinerant frustration: Effects of single-ion anisotropy and bond-dependent anisotropy, *Phys. Rev. B* **103**, 054422 (2021).
- [94] R. Yambe and S. Hayami, Anisotropic spin model and multiple- q states in cubic systems, *Phys. Rev. B* **107**, 174408 (2023).
- [95] R. Yu, M. Yi, B. A. Frandsen, R. J. Birgeneau, and Q. Si, Emergent phases in iron pnictides: Double- Q antiferromagnetism, charge order and enhanced nematic correlations 10.48550/arXiv.1706.07087 (2017).
- [96] S. Hayami, R. Ozawa, and Y. Motome, Effective bilinear-biquadratic model for noncoplanar ordering in itinerant magnets, *Phys. Rev. B* **95**, 224424 (2017).
- [97] Y.-W. Fang, R. Yang, and H. Chen, The complex non-collinear magnetic orderings in Ba_2YO_6 : a new approach to tuning spin-lattice interactions and controlling magnetic orderings in frustrated complex oxides, *Journal of Physics: Condensed Matter* **31**, 445803 (2019).
- [98] S. Paul, S. Haldar, S. von Malottki, and S. Heinze, Role of higher-order exchange interactions for skyrmion stability, *Nature Communications* **11**, 4756 (2020).
- [99] Y. Kato and Y. Motome, Magnetic field-temperature phase diagrams for multiple- Q magnetic ordering: Exact steepest descent approach to long-range interacting spin systems, *Phys. Rev. B* **105**, 174413 (2022).
- [100] S. Hayami, Checkerboard bubble lattice formed by octuple-period quadruple- Q spin density waves, *Phys. Rev. B* **108**, 094415 (2023).
- [101] S. Hayami and R. Yambe, Stabilization mechanisms of magnetic skyrmion crystal and multiple- q states based on momentum-resolved spin interactions, *Materials Today Quantum* **3**, 100010 (2024).
- [102] R. Pohle, N. Shannon, and Y. Motome, Spin nematics meet spin liquids: Exotic quantum phases in the spin-1 bilinear-biquadratic model with Kitaev interactions, *Phys. Rev. B* **107**, L140403 (2023).
- [103] I. Martin and C. D. Batista, Itinerant electron-driven chiral magnetic ordering and spontaneous quantum hall effect in triangular lattice models, *Phys. Rev. Lett.* **101**, 156402 (2008).
- [104] Y. Kato, I. Martin, and C. D. Batista, Stability of the spontaneous quantum hall state in the triangular kondo-lattice model, *Phys. Rev. Lett.* **105**, 266405 (2010).
- [105] R. Ozawa, S. Hayami, and Y. Motome, Zero-field skyrmions with a high topological number in itinerant magnets, *Phys. Rev. Lett.* **118**, 147205 (2017).
- [106] H.-Y. Yang, A. F. Albuquerque, S. Capponi, A. M. Läuchli, and K. P. Schmidt, Effective spin couplings in the Mott insulator of the honeycomb lattice Hubbard model, *New Journal of Physics* **14**, 115027 (2012).
- [107] N. Swain, R. Tiwari, and P. Majumdar, Mott-hubbard transition and spin-liquid state on the pyrochlore lattice, *Phys. Rev. B* **94**, 155119 (2016).
- [108] S. Kawarazaki, K. Fujita, K. Yasuda, Y. Sasaki, T. Mizusaki, and A. Hirai, Direct Evidence for Triple- Q Spin-Density Wave in fcc Antiferromagnetic Mn-Ni Alloy, *Phys. Rev. Lett.* **61**, 471 (1988).
- [109] E. M. Forgan, B. D. Rainford, S. L. Lee, J. S. Abell, and Y. Bi, The magnetic structure of CeAl_2 is a non-chiral spiral, *Journal of Physics: Condensed Matter* **2**, 10211 (1990).
- [110] P. S. Normile, W. G. Stirling, D. Mannix, G. H. Lander, F. Wastin, J. Rebizant, F. Boudarot, P. Burlet, B. Lebech, and S. Coburn, $(\text{U}_{1-x}\text{Pu}_x)\text{Sb}$ solid solutions. I. Magnetic configurations, *Phys. Rev. B* **66**, 014405 (2002).
- [111] E. M. Forgan, E. P. Gibbons, K. A. McEwen, and D. Fort, Observation of a Quadruple- q Magnetic Structure in Neodymium, *Phys. Rev. Lett.* **62**, 470 (1989).
- [112] L. Yue, X. Ren, T. Han, J. Guo, Z. Wu, Y. Zhang, and Y. Li, Raman scattering study of the tetragonal magnetic phase in $\text{Sr}_{1-x}\text{Na}_x\text{Fe}_2\text{As}_2$: Structural symmetry and electronic gap, *Phys. Rev. B* **96**, 180505 (2017).
- [113] J. Jensen and P. Bak, Spin waves in triple- \vec{q} structures. Application to USb, *Phys. Rev. B* **23**, 6180 (1981).
- [114] P. Burlet, E. Ressouche, B. Malaman, R. Welter, J. P. Sanchez, and P. Vulliet, Noncollinear magnetic structure of MnTe_2 , *Phys. Rev. B* **56**, 14013 (1997).
- [115] P. Park, W. Cho, C. Kim, Y. An, Y.-G. Kang, M. Avdeev, R. Sibille, K. Iida, R. Kajimoto, K. H. Lee, *et al.*, Tetrahedral triple- q magnetic ordering and large spontaneous hall conductivity in the metallic triangular antiferromagnet $\text{Co}_{1/3}\text{TaS}_2$, *Nature Communications* **14**, 8346 (2023).
- [116] P. Park, W. Cho, C. Kim, Y. An, K. Iida, R. Kajimoto, S. Matin, S.-S. Zhang, C. D. Batista, and J.-G. Park, Contrasting dynamical properties of single- q and triple- q magnetic orderings in a triangular lattice antiferromagnet, (2024), arXiv:2410.02180 [cond-mat.str-el].
- [117] Y. Dong, B. Zhang, Y. Cao, H. Guo, W. Ren, A. Zhang, Z. Li, Z. Wei, H. Liu, L. Tang, H. Pang, F. Li, and Z. Li, Simple yet clear local evidence for the tetrahedral triple- Q magnetic ground state in the triangular antiferromagnet $\text{Co}_{1/3}\text{NbS}_2$, *Phys. Rev. B* **109**, 094401 (2024).
- [118] M. N. Gastiasoro, I. Eremin, R. M. Fernandes, and B. M. Andersen, Scanning tunnelling spectroscopy as a probe of multi- Q magnetic states of itinerant magnets, *Nature communications* **8**, 14317 (2017).
- [119] J. Spethmann, S. Meyer, K. von Bergmann, R. Wiesendanger, S. Heinze, and A. Kubetzka, Discovery of Magnetic Single- and Triple- q States in $\text{Mn}/\text{Re}(0001)$, *Phys. Rev. Lett.* **124**, 227203 (2020).
- [120] Y. Tokunaga, Y. Homma, S. Kambe, D. Aoki, H. Sakai, E. Yamamoto, A. Nakamura, Y. Shiokawa, R. E. Walstedt, and H. Yasuoka, NMR Evidence for Triple- \vec{q} Multipole Structure in NpO_2 , *Phys. Rev. Lett.* **94**, 137209 (2005).
- [121] X. Jin, M. Geng, F. Orlandi, D. Khalyavin, P. Manuel, Y. Liu, and Y. Li, Robust triple- q magnetic order with trainable spin vorticity in $\text{Na}_2\text{Co}_2\text{TeO}_6$ (2025), arXiv:2501.07843 [cond-mat.str-el].
- [122] J. Wang and Z.-X. Liu, Effect of ring-exchange interactions in the extended kitaev honeycomb model, *Phys. Rev. B* **108**, 014437 (2023).
- [123] T. Shimokawa, T. Okubo, and H. Kawamura, Multiple- q states of the $J_1 - J_2$ classical honeycomb-lattice heisenberg antiferromagnet under a magnetic field, *Phys. Rev. B* **100**, 224404 (2019).
- [124] W. Yao and Y. Li, Ferrimagnetism and Anisotropic Phase Tunability by Magnetic Fields in $\text{Na}_2\text{Co}_2\text{TeO}_6$, *Phys. Rev. B* **101**, 085120 (2020).
- [125] P. Miao, X. Jin, W. Yao, Y. Chen, A. Koda, Z. Tan, W. Xie, W. Ji, T. Kamiyama, and Y. Li, Persistent spin

- dynamics in magnetically ordered honeycomb-lattice cobalt oxides, *Phys. Rev. B* **109**, 134431 (2024).
- [126] W. Yao, K. Iida, K. Kamazawa, and Y. Li, Excitations in the Ordered and Paramagnetic States of Honeycomb Magnet $\text{Na}_2\text{Co}_2\text{TeO}_6$, *Phys. Rev. Lett.* **129**, 147202 (2022).
- [127] G. Lin, J. Jeong, C. Kim, Y. Wang, Q. Huang, T. Masuda, S. Asai, S. Itoh, G. Günther, M. Russina, *et al.*, Field-induced quantum spin disordered state in spin-1/2 honeycomb magnet $\text{Na}_2\text{Co}_2\text{TeO}_6$, *Nature communications* **12**, 5559 (2021).
- [128] C. Kim, J. Jeong, G. Lin, P. Park, T. Masuda, S. Asai, S. Itoh, H.-S. Kim, H. Zhou, J. Ma, and J.-G. Park, Antiferromagnetic Kitaev interaction in $\text{Jeff} = 1/2$ cobalt honeycomb materials $\text{Na}_3\text{Co}_2\text{SbO}_6$ and $\text{Na}_2\text{Co}_2\text{TeO}_6$, *Journal of Physics: Condensed Matter* **34**, 045802 (2021).
- [129] Y. Singh, S. Manni, J. Reuther, T. Berlijn, R. Thomale, W. Ku, S. Trebst, and P. Gegenwart, Relevance of the Heisenberg-Kitaev Model for the Honeycomb Lattice Iridates A_2IrO_3 , *Phys. Rev. Lett.* **108**, 127203 (2012).
- [130] L. Janssen, E. C. Andrade, and M. Vojta, Honeycomb-Lattice Heisenberg-Kitaev Model in a Magnetic Field: Spin Canting, Metamagnetism, and Vortex Crystals, *Phys. Rev. Lett.* **117**, 277202 (2016).
- [131] G.-W. Chern, Y. Sizyuk, C. Price, and N. B. Perkins, Kitaev-heisenberg model in a magnetic field: Order-by-disorder and commensurate-incommensurate transitions, *Phys. Rev. B* **95**, 144427 (2017).
- [132] S. M. Winter, Magnetic couplings in edge-sharing high-spin d^7 compounds, *Journal of Physics: Materials* **5**, 045003 (2022).
- [133] C. Wellm, W. Roscher, J. Zeisner, A. Alfonsov, R. Zhong, R. J. Cava, A. Savoyant, R. Hayn, J. van den Brink, B. Büchner, O. Janson, and V. Kataev, Frustration enhanced by Kitaev exchange in a $j_{\text{eff}} = \frac{1}{2}$ triangular antiferromagnet, *Phys. Rev. B* **104**, L100420 (2021).
- [134] H. S. Nair, J. M. Brown, E. Coldren, G. Hester, M. P. Gelfand, A. Podlesnyak, Q. Huang, and K. A. Ross, Short-range order in the quantum XXZ honeycomb lattice material $\text{BaCo}_2(\text{PO}_4)_2$, *Phys. Rev. B* **97**, 134409 (2018).
- [135] P. A. Maksimov, A. V. Ushakov, Z. V. Pchelkina, Y. Li, S. M. Winter, and S. V. Streltsov, Ab initio guided minimal model for the “Kitaev” material $\text{BaCo}_2(\text{AsO}_4)_2$: Importance of direct hopping, third-neighbor exchange, and quantum fluctuations, *Phys. Rev. B* **106**, 165131 (2022).
- [136] N. Francini and L. Janssen, Spin vestigial orders in extended Heisenberg-Kitaev models near hidden $\text{SU}(2)$ points: Application to $\text{Na}_2\text{Co}_2\text{TeO}_6$, *Phys. Rev. B* **109**, 075104 (2024).
- [137] N. Francini and L. Janssen, Ferrimagnetism from triple-q order in $\text{Na}_2\text{Co}_2\text{TeO}_6$, *Phys. Rev. B* **110**, 235118 (2024).
- [138] J. Merino and A. Ralko, Role of quantum fluctuations on spin liquids and ordered phases in the heisenberg model on the honeycomb lattice, *Phys. Rev. B* **97**, 205112 (2018).
- [139] Z. Zhu and S. R. White, Quantum phases of the frustrated xy models on the honeycomb lattice, *Modern Physics Letters B* **28**, 1430016 (2014).
- [140] R. F. Bishop, P. H. Y. Li, D. J. J. Farnell, and C. E. Campbell, The frustrated Heisenberg antiferromagnet on the honeycomb lattice: $J_1 - J_2$ model, *Journal of Physics: Condensed Matter* **24**, 236002 (2012).
- [141] A. Bose, M. Routh, S. Voleti, S. K. Saha, M. Kumar, T. Saha-Dasgupta, and A. Paramekanti, Proximate Dirac spin liquid in the honeycomb lattice $J_1 - J_3$ XXZ model: Numerical study and application to cobaltates, *Phys. Rev. B* **108**, 174422 (2023).
- [142] L. Y. Shi, X. M. Wang, R. D. Zhong, Z. X. Wang, T. C. Hu, S. J. Zhang, Q. M. Liu, T. Dong, F. Wang, and N. L. Wang, Magnetic excitations of the field-induced states in $\text{BaCo}_2(\text{AsO}_4)_2$ probed by time-domain terahertz spectroscopy, *Phys. Rev. B* **104**, 144408 (2021).
- [143] X. Zhang, Y. Xu, T. Halloran, R. Zhong, C. Broholm, R. Cava, N. Driehko, and N. Armitage, A magnetic continuum in the cobalt-based honeycomb magnet $\text{BaCo}_2(\text{AsO}_4)_2$, *Nature Materials* **22**, 58 (2023).
- [144] J. Jiao, X. Li, G. Lin, M. Shu, W. Xu, O. Zaharko, T. Shiroka, T. Hong, A. I. Kolesnikov, G. Deng, *et al.*, Static magnetic order with strong quantum fluctuations in spin-1/2 honeycomb magnet $\text{Na}_2\text{Co}_2\text{TeO}_6$, *Communications Materials* **5**, 159 (2024).
- [145] E. Lefrançois, G. Grissonnanche, J. Baglo, P. Lampen-Kelley, J.-Q. Yan, C. Balz, D. Mandrus, S. E. Nagler, S. Kim, Y.-J. Kim, N. Doiron-Leyraud, and L. Taillefer, Evidence of a Phonon Hall Effect in the Kitaev Spin Liquid Candidate $\alpha\text{-RuCl}_3$, *Phys. Rev. X* **12**, 021025 (2022).
- [146] E. Lefrançois, J. Baglo, Q. Barthélemy, S. Kim, Y.-J. Kim, and L. Taillefer, Oscillations in the magnetothermal conductivity of $\alpha - \text{RuCl}_3$: Evidence of transition anomalies, *Phys. Rev. B* **107**, 064408 (2023).
- [147] J. Sears, Y. Shen, M. J. Krogstad, H. Miao, J. Yan, S. Kim, W. He, E. S. Bozin, I. K. Robinson, R. Osborn, S. Rosenkranz, Y.-J. Kim, and M. P. M. Dean, Stacking disorder in $\alpha\text{-RuCl}_3$ investigated via x-ray three-dimensional difference pair distribution function analysis, *Phys. Rev. B* **108**, 144419 (2023).
- [148] X. Hong, M. Gillig, W. Yao, L. Janssen, V. Kocsis, S. Gass, Y. Li, A. U. Wolter, B. Büchner, and C. Hess, Phonon thermal transport shaped by strong spin-phonon scattering in a Kitaev material $\text{Na}_2\text{Co}_2\text{TeO}_6$, *npj Quantum Materials* **9**, 18 (2024).
- [149] H. Takeda, J. Mai, M. Akazawa, K. Tamura, J. Yan, K. Moovendaran, K. Raju, R. Sankar, K.-Y. Choi, and M. Yamashita, Planar thermal Hall effects in the Kitaev spin liquid candidate $\text{Na}_2\text{Co}_2\text{TeO}_6$, *Phys. Rev. Res.* **4**, L042035 (2022).